papers and notes on methodology

Identifying the predominant peak diameter of high-density and low-density lipoproteins by electrophoresis

Paul T. Williams, Ronald M. Krauss, Alex V. Nichols, Karen M. Vranizan, and Peter D. S. Wood

Division of Research Medicine and Radiation Biophysics, Lawrence Berkeley Laboratory. 1 Cyclotron Road, Bldg. 934, Berkeley, CA 94720, and Stanford Center for Research in Disease Prevention, Stanford University Medical Center, Stanford, CA 94720

Abstract Particle size distributions of high-density (HDL) and low-density (LDL) lipoproteins, obtained by polyacrylamide gradient gel electrophoresis, exhibit apparent predominant and minor peaks within characteristic subpopulation migration intervals. In the present report, we show that identification of such peaks as predominant or minor depends on whether the particle size distribution is analyzed according to migration distance or particle size. The predominant HDL peak on the migration distance scale is frequently not the predominant HDL peak when the distribution is transformed to the particle size scale. The potential physiologic importance of correct identification of the predominant HDL peak within a gradient gel electrophoresis profile is suggested by our cross-sectional study of 97 men, in which diameters associated with the predominant peak, determined using migration distance and particle size scales, were correlated with plasma lipoprotein and lipid parameters. Plasma concentrations of HDL-cholesterol, triglycerides, and apolipoproteins A-I and B correlated more strongly with the predominant peak obtained using the particle size scale than the migration distance scale. The mathematical transformation from migration distance to particle diameter scale had less effect on the LDL distribution. The additional computational effort required to transform the HDL-distribution into the particle size scale appears warranted given the substantial changes it produces in the gradient gel electrophoresis profile and the strengthening of correlations with parameters relevant to lipoprotein metabolism.—**Williams, P. T., R. M. Krauss, A. V. Nichols, K. M. Vranizan, and P. D. S. Wood.** Identifying the predominant peak diameter of high-density and low-density lipoproteins by electrophoresis. *J. Lipid Res.* 1990. **31:** 1131-1139.

Supplementary key words gradient gel electrophoresis • lipoproteins • HDL • LDL

Several subclasses of high-density (HDL) and low-density lipoproteins (LDL) have been identified by their electrophoretic mobility on polyacrylamide gradient gels (1, 2). The gels act as continuous molecular sieve gradients that essentially exclude larger particles from migrating further down the gels. The variations in absorbances of the gels stained for protein reveal the relative concentrations of HDL and LDL-protein at characteristic migration distances (R_f). These densitometric displays of the HDL and LDL distributions include modes and inflection points that are assumed to correspond to lipoprotein subclasses. Five HDL subclasses and seven LDL subclasses have been defined by this method (1, 2).

The apparent particle size distributions of HDL and LDL protein are affected by the physical characteristics of the polyacrylamide gels. The pore diameters decrease nonlinearly along the gel. The curvilinear relationship between migration distance and pore diameters distorts the shapes of the distributions. This may even produce inflection points, maxima and minima that are artifacts of the gel's nonlinearity.

These distortions may be corrected in part by mathematically transforming the entire lipoprotein distribution from the migration distance scale into the diameter scale. This simple transformation makes two assumptions: *1*) the migration distances of the protein standards are due to exclusion by size; and *2*) lipoprotein particles are excluded by the same criteria as the protein standards. Although other factors affect protein and lipoprotein migration distances, the distances traveled on the gels primarily reflect exclusion by particle size. This report examines the effects of this mathematical transformation on the shape of the HDL and LDL distributions.

Abbreviations: HDL, high density lipoproteins: LDL, low density lipoproteins.

METHODS

Subjects

The study group was comprised of 97 of 155 sedentary men who were recruited to participate in a 1-year study of diet and exercise (3). The men were 30–59 years old, 20- 60% over Metropolitan ideal weight (4), nonsmokers, not on medication that might affect lipid metabolism, nonhypertensive (blood pressure < 160/100 mm Hg), and nonhyperlipidemic (plasma total cholesterol <8.28 mmol/l and triglycerides <5.65 mmol/l). The men reported to our clinic in the morning, having abstained for 12–16 h from all food and any vigorous activity. Blood samples were collected in EDTA (1 mg/l) after an overnight fast (3).

Laboratory methods

Plasma lipoprotein cholesterol concentrations were measured directly by the methods of the Lipid Research Clinics (5), plasma apolipoprotein B concentrations were assessed by radioimmunoassay (6), and apolipoprotein A-I and A-II concentrations were measured by radialimmunodiffusion (7). Fasting lipoprotein cholesterol concentrations were determined by the methods of the Lipid Research Clinics (8).

Electrophoresis of HDL in the ultracentrifuged d $\leq$ 1.20 g/ml fraction was done on Pharmacia Electrophoresis Apparatus (GE 4-11) using slab gradient gels (PAA 4/30, Pharmacia, Piscataway, NJ) as described by Blanche et al. (1). The protein-stained gradient gels were scanned with a model RFT densitometer (Transidyne Corp., Ann Arbor, MI) at a wave length of 603 nm. A mixture of four globular proteins (HMW Calibration Kit) was run on the central lane to calibrate for particle size. The HDL-migration distances (R_f) were measured relative to the migration distance of the peak of bovine serum albumin, one of the protein standards. A known concentration of thyroglobulin (0.35 mg/ml) was applied to each HDL sample to correct for differences in sample volume and stain uptake. Five HDL subclasses are suggested by this method: HDL_{3c} (7.2–7.8 nm), HDL_{3b} (7.8–8.2 nm), HDL_{3a} (8.2–8.8 nm), HDL_{2a} (8.8–9.7 nm), and HDL_{2b} (9.7–12.9 nm).

Electrophoresis of LDL was done using Pharmacia 2–16% polyacrylamide gradient gels as described by Krauss and Burke (2). LDL-migration distances (R_f) were measured relative to apoferritin.

Converting migration distance into particle diameter

A quadratic equation was used to convert migration distance (R_f) into hydrated particle diameter (nm). The equation was obtained by standard polynomial regression of Stoke's diameter versus migration distances of four standard proteins. HDL-diameters were estimated from thyroglobulin (17.0 nm), apoferritin (12.2 nm), lactate dehydrogenase (8.16 nm), and bovine serum albumin (7.1 nm). LDL-diameters were estimated from the migration distances of latex beads (38.0 nm), thyroglobulin dimer (23.6 nm), thyroglobulin (17.0 nm), and apoferritin (12.2 nm). The hydrated molecular diameters are transformed to their natural logarithms for these calculations, i.e.:

$$\text{Diameter} = \exp\{\alpha + \beta R_f + \eta R_f^2\} \qquad Eq\ 1)$$

By completing the square in equation 1, we can also obtain the equation for converting molecular diameter (nm) to migration distance (R_f):

$$R_f = \frac{-\beta - \{4\eta(\text{Ln}(\text{Diameter}) - \alpha) + \beta^2\}^{1/2}}{2\eta} \qquad Eq.\ 2)$$

Fig. 1 shows the functions for converting migrating distances into HDL and LDL hydrated particle diameters for one of the 97 subjects in our sample (ID#99). The curvature of the function is greater for HDL than LDL.

Converting the HDL and LDL distributions into particle diameter

Equation 1 gives the molecular diameter for a specific migration distance. The conversion of the entire HDL or LDL distribution from migration distance to diameter is more complicated. It involves a change in both the height

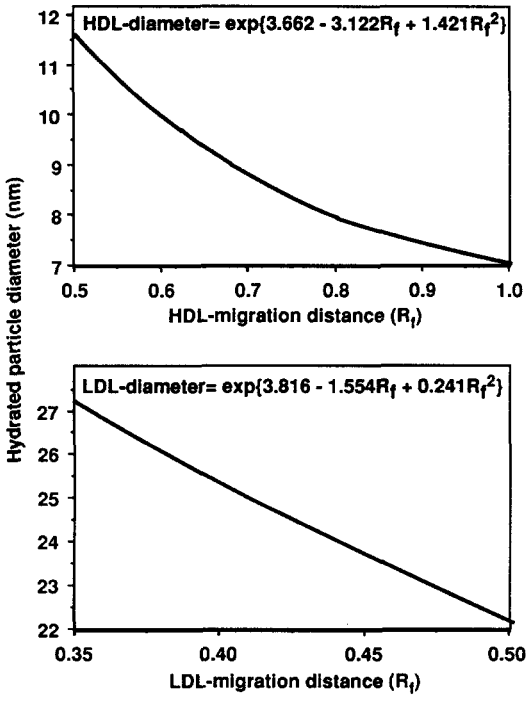

Fig. 1. Examples of the functions $g(R_f)$ that convert HDL and LDL migration distances into estimated hydrated particle diameters.

of the curve along the the y-axis and the scale of the distribution along the x-axis.

Converting the total HDL and LDL distributions into particle diameter is mathematically the same problem as obtaining the probability distribution for a tranformed variable (9). Let:

$f(R_f)$ be the lipoprotein distribution as plotted against migration distance;

$g(R_f)$ be the function that converts migration distance into particle diameter (equation 1, Fig. 1)

g^{-1}(Diameter) be the function that converts particle diameter into migration distance (equation 2, **Fig. 2**).

The lipoprotein distribution as plotted against particle diameter is simply:

$$f(g^{-1}(\text{Diameter})) \left| \frac{dg^{-1}(\text{Diameter})}{d\text{Diameter}} \right| \qquad \text{Eq. 3)}$$

where

$$\left| \frac{dg^{-1}(\text{Diameter})}{d\text{Diameter}} \right| = \qquad \text{Eq. 4)}$$

$$\left| \text{Diameter}^{-1} \{4\eta[\text{Ln}(\text{Diameter}) - \alpha] + \beta^2\}^{-1/2} \right|$$

The transformation may be simply stated: at each migration distance (R_f), we obtain the diameter from equation 1, and then multiply the height of the distribution by the value of equation 4.

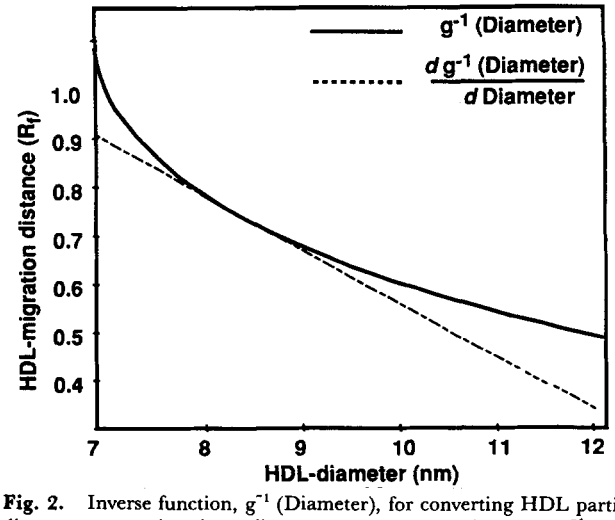

Fig. 2. Inverse function, g^{-1} (Diameter), for converting HDL particle diameter to migration distance, and its derivative dg^{-1} (Diameter)/dDiameter. Their formulae are given in equations 3 and 4, respectively.

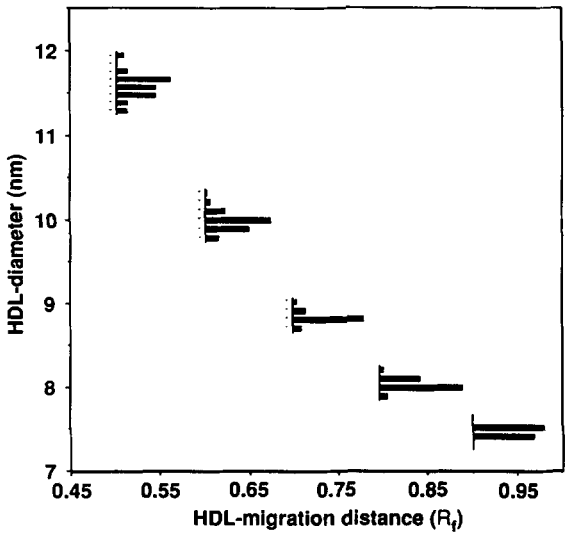

Fig. 3. Histograms of the estimated hydrated particle diameters for selected HDL-migration distances in 97 men.

RESULTS

Eliminating variation between gels

The calibration curves remove some of the variation between gels. Different coefficients for these curves are obtained for each gel, i.e., the relationship between migration distance and particle diameter is gel specific. To illustrate this point, we calculated the coefficients of equation 1 for the gels of the 97 men. These coefficients were then used to estimate the diameters that correspond to R_f values of 0.5, 0.6, 0.7, 0.8, 0.9 in each man. **Fig. 3** displays the histogram for the 97 diameters at each R_f value. The length of each bar shows the proportion of the 97 diameters that fall within each 0.1-nm interval. The histograms show that the variation is greatest at lower migration distances, i.e., within the HDL_2 interval, and least at the higher migration distances, i.e., within the HDL_{3c} interval. These results suggest that the precision of the migration distance scale may be greater within the HDL_3 than within the HDL_2 interval.

Changes in the high-density lipoprotein distribution

Area is conserved when the distribution is converted into particle diameter. Equation 3 does not affect the area under the curve. The area under the curve between any two R_f values is the same as the area under the curve for their corresponding diameters (9).

The shape of the distribution is not conserved when the distribution is converted into particle diameter. **Fig. 4** displays the average distribution of HDL by migration distance (top) and by particle diameter (bottom) for the 97 men. These distributions were produced by averaging the heights of the 97 separate HDL-distributions at each point. Both distributions display peaks within the HDL_{3b}, HDL_{3a}, and

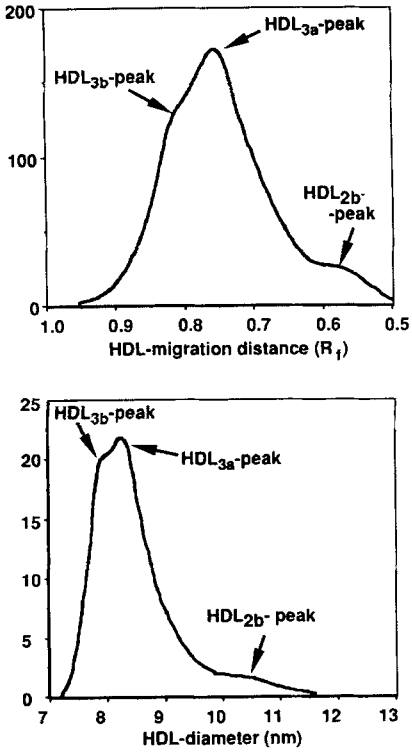

Fig. 4. Mean distribution of HDL plotted against migration distance and particle diameter in 97 men. (Note: the axis of the migration distance scale goes from larger to smaller R_f values to correspond to the diameter scale.)

HDL_{2b} size intervals. These occur at R_f values of approximately 0.81 (within the HDL_{3b} interval), 0.76 (HDL_{3a} interval), and 0.57 (HDL_{2b} interval) when plotted against migration distance, and at approximately 7.9, 8.3, and 10.3 nm, respectively, when plotted against diameter.

The transformation changes the distribution of HDL along the x-axis. As shown in Fig. 4, the HDL_{2a+3} interval occupies a smaller proportion of the total HDL range when plotted against diameter (approximately 7.2 to 9.7 nm) than when plotted against migration distance (approximately R_f 0.627 to 0.962). Correspondingly, HDL_{2b} occupies a greater proportion of the total HDL region when plotted against diameter. These changes are the result of the nonlinear relationship between pore size and migration distance.

Transforming the HDL distribution from the migration distance scale into the diameter scale also changes the height of the HDL-distribution. The effect will vary for different values, further changing the shape of the distribution. The transformation increases the relative height of the HDL_3 peaks as compared to the HDL_2 peak, and increases the relative height of the HDL_{3b} peak as compared to the HDL_{3a} peak (Fig. 4). These changes are brought about when the heights of the HDL-distribution are multiplied by equation 4.

Subject #99's data illustrate the effect of the transformation. **Fig. 5** presents his HDL-distribution by migration distance (top) and particle diameter (bottom). Fig. 1 shows the mathematical function for changing his migration distances to particle diameters, and Fig. 2 shows the inverse of this function and its derivative. The portion of Fig. 1 that falls between 7.6 and 8.8 nm is reproduced in **Fig. 6**.

Finally, we need to establish several definitions: *Predominant HDL-peak migration distance* refers to the location of the highest point of the total HDL distribution when plotted against the migration distance scale. *Apparent predominant HDL-peak diameter* refers to the diameter that corresponds to the HDL-peak migration distance (i.e., the diameter of the peak as determined from Fig. 1). Let *the true predominant HDL-peak diameter* refer to the location of the highest point of the total HDL-distribution when plotted against the diameter scale.

Subject 99's predominant HDL-peak migration distance occurs in the HDL_{3a} interval at R_f 0.741 (Fig. 5, top); its height is 189.3 scanning units. As shown in Fig. 1, a migration distance of R_f 0.741 corresponds to a diameter of 8.41 nm. However, the predominant HDL-peak diameter measured directly is not 8.41 nm (Fig. 5, bottom). Plotting the HDL-distribution by particle size shows that the true predominant peak diameter is 7.89 nm in the HDL_{3b} interval. This peak appears in the

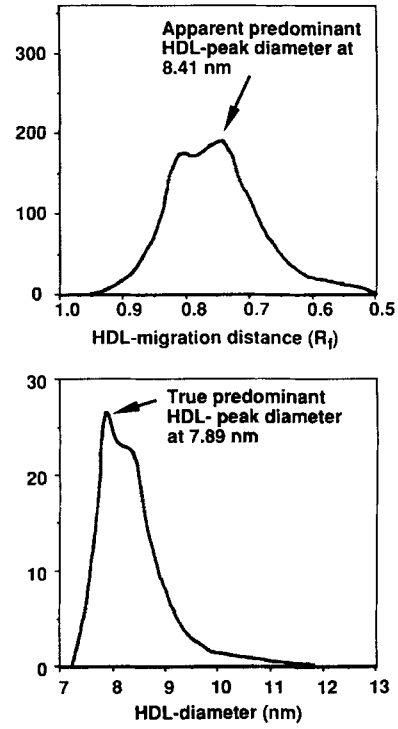

Fig. 5. An example showing that the predominant HDL peak can change from the HDL_{3a} interval to the HDL_{3b} interval when the HDL distribution is transformed from the migration distance to diameter scale.

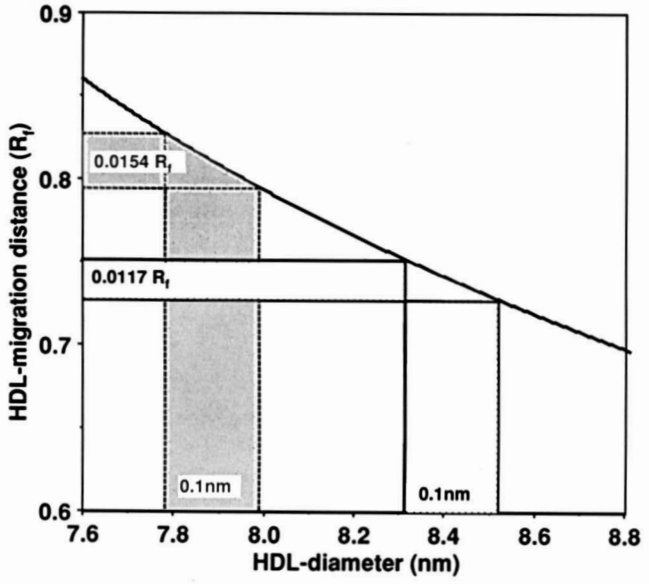

Fig. 6. When plotted against migration distance, an interval of 0.1 nm is compressed into a smaller interval at 8.41 nm (within HDL_{3a}) than at 7.89 nm (within HDL_{3b}).

migration distance scale as a minor peak at R_f 0.809, and has a height of 172.3 scanning units.

The apparent predominant HDL-peak diameter (8.41 nm) differs from the true HDL-peak diameter (7.89 nm) because the transformation involves a nonlinear change in scale along the horizontal (x) axis. The height of the HDL distribution must be adjusted accordingly. The adjustment is given by equation 4 and is illustrated in Fig. 6. Because the curve in Fig. 6 is not a straight line, the change in scale will be different at different points along the horizontal axis. The tangent to the function in Fig. 6 will become more steep as the diameter decreases. In other words, when plotted against migration distance, an interval of 0.1 nm is compressed less in the HDL_{3b} than in the HDL_{3a} interval.

The computations leading to this result are as follows: for subject #99, at R_f 0.741, equation 4 gives a value of 0.117 scanning units. The height of the HDL distribution on the migration distance scale (189.5) must therefore be multiplied by 0.117 to obtain its height on the diameter scale. The height of the HDL distribution at 8.41 nm is therefore:

$$189.5 \times 0.117 = 22.1 \text{ scanning units.}$$

At 0.81 R_f, the value of equation 4 is 0.154. The height of the HDL-distribution at 7.89 nm is therefore:

$$172.3 \times 0.154 = 26.5 \text{ scanning units}$$

which is greater than 22.1. This leads to the following result.

The apparent peak diameter often overestimates the true predominant HDL-peak diameter. In Fig. 5, we showed one example where the apparent peak diameter overestimates the size of the true predominant HDL-peak. This occurs frequently. **Fig. 7** compares the apparent peak diameter (horizontal axis) with the true predominant peak diameter (vertical axis) in a cross-sectional study of 97 men. All of the points lie either on or below the diagonal. This means that the apparent diameter was always greater than or equal to the true peak diameter. Many cases having their apparent predominant peak diameter in the HDL_{3a} interval are found to have their true predominant peak diameter in HDL_{3b} interval. According to the apparent peak diameters, only 14 (14.4%) men have their predominant peak in the HDL_{3b} interval. In contrast, indentifying the predominant peak diameter directly shows that 42 men (43%) have their predominant peak in the HDL_{3b} interval. Thus 28 men (29%) were misclassified as having their predominant peak in the HDL_{3a} interval by the apparent diameter.

Fig. 8 displays the HDL distribution of one man (not part of the baseline sample of 97 men) whose predominant HDL peak on the migration distance scale occurs in the HDL_{2b} interval. His HDL_{2b} had been elevated after following an exercise regimen for 7 months. Transforming his HDL-distribution into the diameter scale shifts the predominant peak from the HDL_{2b} interval to the HDL_{3a} interval. When plotted against migration distance, the HDL_{2b} interval is even more compressed than either the HDL_{3a} or HDL_{3b} intervals.

Other lipoprotein measurements correlate more strongly with the true predominant HDL peak diameter than with the apparent predominant HDL-peak diameter. The possible physiological

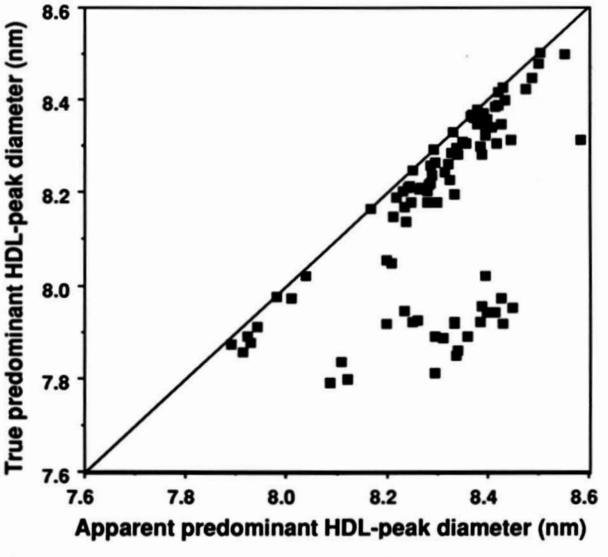

Fig. 7. Scatterplot showing that the apparent HDL peak diameter frequently overestimates the true HDL peak diameter.

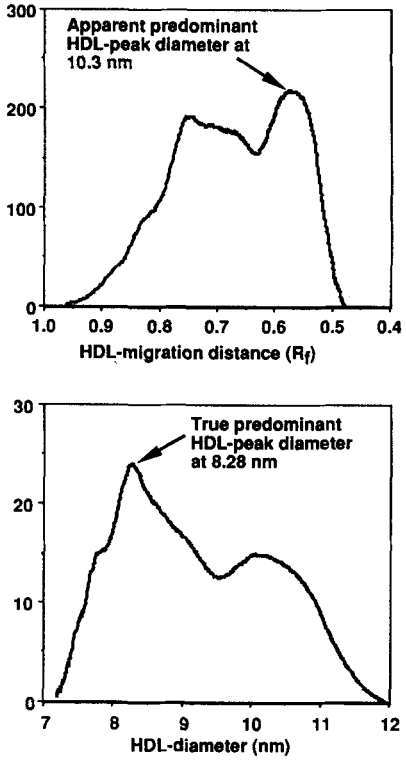

Fig. 8. An example showing that the predominant HDL peak can change from the HDL_{2b} region to the HDL_{3a} region by transforming the HDL distribution from the migration distance to diameter scale.

relevance of the two predominant peak diameter measurements was evaluated by comparing their relationships to other lipoproteins. **Table 1** displays the Pearson correlation coefficient between various lipoproteins and *1*) the true predominant HDL-peak diameter and *2*) the apparent predominant HDL-peak diameter. The apparent and true predominant HDL-peak diameters were each negatively correlated with plasma triglyceride and apolipoprotein B concentrations and positively correlated with HDL-cholesterol and apolipoprotein A-I concentrations and the size of the predominant LDL peak. In almost all cases, the correlations were stronger for the true than for the apparent HDL-peak diameter. When both the true and the apparent HDL-peak diameter were included in multiple regression analyses (**Table 2**), the true diameter significantly predicted plasma triglycerides, HDL-cholesterol, and apolipoprotein B concentrations and LDL-peak diameter, whereas the apparent peak diameters usually did not. Thus the true diameter is significantly related to these lipoprotein measurements after adjustment for the apparent diameter.

Table 3 displays the mean plasma lipoprotein concentrations for men divided into two groups: those with a predominant HDL_{3a} peak and those with a predominant HDL_{3b} peak, as determined on both scales. Men with a predominant HDL_{3b} peak had higher plasma triglyceride and apolipoprotein B concentrations, lower HDL-cholesterol and apolipoprotein A-I levels, and smaller predominant LDL peaks than men with a predominant HDL_{3a} peak. For essentially all variables, the significance of the mean difference was greater when classified by the true peak diameter than by the apparent peak diameter. The apolipoprotein A-I and B differences were, *in fact, not* significant when the men were classified by their apparent diameter.

The significance of the mean difference was also usually greater when classified by the true predominant peak diameter than when classified by the areas of the interval estimates of the HDL subclasses (1). Thirteen men had a greater portion of their HDL within the HDL_{3b} interval than within the HDL_{3a} interval; 11 had their true predominant peak in the 3b region; and 10 had their apparent peak in the 3b region. When compared to the remaining 84 men, the significance of their mean lipoprotein differences was similar to those reported in Table 3 for the apparent peak diameter: triglycerides ($P < 0.003$), HDL-cholesterol ($P = 0.05$), LDL-cholesterol ($P = 0.25$), apolipoprotein A-I ($P = 0.85$), apolipoprotein A-II ($P = 0.30$), apolipoprotein B ($P = 0.04$), and LDL-peak particle diameter ($P = 0.01$).

TABLE 1. Pearson correlation coefficients of the true and the apparent predominant HDL peak diameter versus lipids and apolipoproteins in 97 men

		Correlation with:	
	Mean ± Standard Deviation	True Predominant HDL-Peak Diameter	Apparent Predominant HDL-Peak Diameter
Triglycerides (mg/dl)	138.2 ± 67.4	−0.48****	−0.38****
HDL-cholesterol (mg/dl)	44.5 ± 9.4	0.44****	0.40****
LDL-cholesterol (mg/dl)	153.0 ± 33.6	−0.18	−0.12
Apolipoprotein A-I (mg/dl)	139.3 ± 21.3	0.26**	0.24*
Apolipoprotein A-II (mg/dl)	31.6 ± 5.5	0.07	0.10
Apolipoprotein B (mg/dl)	130.5 ± 31.5	−0.31**	−0.24*
LDL peak particle diameter (nm)	25.82 ± 0.79	0.46****	0.39****

Significance levels for Pearson correlation coefficients are coded: *$P < 0.05$; **$P < 0.01$; ***$P < 0.001$; and ****$P < 0.0001$.

TABLE 2. Multiple regression analyses of plasma triglycerides, HDL-cholesterol, and apolipoprotein B concentrations, and true LDL-peak diameter in 97 men

	Dependent Variables			
Independent Variables	Triglycerides	HDL Cholesterol	ApoB	LDL Peak Diameter
Intercept	1808.2	−208.9	60.7	561.8
True HDL-peak diameter	−13.8***	1.5**	1.4**	−4.2*
Apparent HDL-peak diameter	−6.5	1.5*	1.0	−1.1

Significance levels for regression correlation are coded: $^{*}P < 0.05$; $^{**}P < 0.01$; $^{***}P < 0.001$; and $^{****}P < 0.0001$.

Changes in the low-density lipoprotein distribution

The conversion from migration distance to particle diameter has less effect on the LDL distribution than on the HDL distribution. Fig. 1 shows that the function for converting from the migration distance scale to the particle diameter scale is less curved for LDL between 22.0 and 27.2 nm than for HDL between 7.2 and 12.0 nm. In addition, the major peak of the LDL distribution is often sharp, as shown in **Fig. 9** for subject #99. For these two reasons, there is usually exact corespondence between the true and the apparent predominant LDL-peak diameter. This is shown in **Fig. 10**, where 95 of the 97 men fall along the diagonal. The apparent peak diameter overestimated the true predominant peak diameter in only two cases. These two LDL distributions were both bimodal, with the height of the larger particle only slightly favored when plotted against migration distance.

DISCUSSION

The conversion from migration distance to particle diameter scale removes some of the variation between gels,

TABLE 3. Mean lipid and lipoprotein differences between men with predominant HDL_{3a} and HDL_{3b} peaks as classified by the true and the apparent predominant HDL-peak diameter

	Predominant HDL_{3b}-Peak Mean ± SD	Predominant HDL_{3a}-Peak Mean ± SD	Difference ± SE	Significance
Triglycerides (mg/dl)				
Classified by true peak	172.5 ± 74.8	112.1 ± 47.2	60.4 ± 13.2	0.0001
Classified by apparent peak	204.8 ± 73.9	127.0 ± 59.8	77.8 ± 20.8	0.002
HDL-cholesterol (mg/dl)				
Classified by true peak	40.6 ± 7.7	47.5 ± 9.5	−6.9 ± 1.7	0.0002
Classified by apparent peak	39.3 ± 10.2	45.4 ± 9.0	−6.1 ± 2.9	0.05
LDL-cholesterol (mg/dl)				
Classified by true peak	156.0 ± 31.4	150.7 ± 35.3	5.3 ± 6.8	0.43
Classified by apparent peak	164.8 ± 35.9	151.0 ± 33.0	13.8 ± 10.2	0.20
Apolipoprotein A-I (mg/dl)				
Classified by true peak	133.0 ± 17.3	144.0 ± 23.0	−11.0 ± 4.1	0.01
Classified by apparent peak	139.1 ± 15.4	139.3 ± 22.2	−0.2 ± 4.8	0.97
Apolipoprotein A-II (mg/dl)				
Classified by true peak	31.1 ± 4.8	31.9 ± 6.1	−0.8 ± 1.1	0.49
Classified by apparent peak	31.7 ± 5.6	31.5 ± 5.6	0.2 ± 1.6	0.90
Apolipoprotein B (mg/dl)				
Classified by true peak	138.0 ± 34.6	124.6 ± 27.7	13.4 ± 6.5	0.04
Classified by apparent peak	145.2 ± 44.1	128.0 ± 28.4	17.2 ± 12.2	0.18
LDL peak particle diameter (nm)				
Classified by true peak	25.44 ± 0.77	26.10 ± 0.69	−0.66 ± 0.15	0.0001
Classified by apparent peak	25.26 ± 0.87	25.91 ± 0.74	−0.65 ± 0.25	0.02
Sample size				
Classified by true peak	42	55		
Classified by apparent peak	14	83		

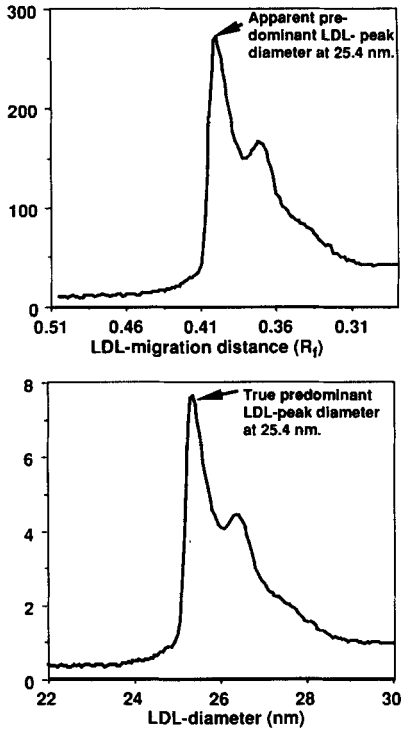

Fig. 9. In most cases, the diameter equivalents of the LDL-peak migration distance and the LDL-peak diameter are the same, as in this example.

but this is not our purpose for transforming the data. Our purpose is to obtain a depiction of the lipoprotein distributions with characteristics that primarily reflect the heterogeneity of HDL and LDL structure. As depicted on the gradient gels, the lipoprotein distributions appear as the convolution of two mathematical functions: *1*) the distribution of HDL and LDL-protein by particle diameter; and *2*) the relationship between particle diameter and migration distance. The first function is a property of the HDL and LDL particles themselves and is presumably an important feature of their structure; the second is a property of the gradient gel and is biologically irrelevant. Transforming the HDL distribution and the LDL distribution from migration distance to particle diameter removes the irrelevant relationship between particle diameter and migration distance.

Nondenaturing gradient gel electrophoresis provides greater resolution of high-density and low-density lipoprotein subclasses than analytic ultracentrifugation (1, 2). The shape of the lipoprotein distribution is a key characteristic for identifying these subclasses on the gradient gel. This includes the number, location, and relative heights of the modes (peaks) and shoulders. However, their unqualified use can be misleading, particularly for analyses of HDL subfractions. This is because the distribution of stained protein is distorted by the curvilinear relationship between pore diameter and migration distance, causing larger particles to be compressed into a smaller interval on the gel. This means that the direct scans of the gels overemphasize the prominance of the HDL_{2b} and HDL_{3a} peaks and underemphasize the HDL_{3b} and HDL_{3c} peaks. The distortion is eliminated by a simple mathematical transformation. To our knowledge, the study by Chen et al. (10) is the only analysis to determine the diameter of the predominant HDL peak directly.

In addition to being mathematically correct, the transformed distribution also appears to have greater biological relevance. Plasma concentrations of HDL-cholesterol, triglycerides, apolipoproteins A-I and B, and LDL-peak particle diameter were all correlated more strongly with the true predominant HDL-peak diameter, than with its apparent peak diameter. Moreover, the significance of the lipoprotein differences between men with a predominant HDL_{3a} peak and those with a predominant HDL_{3b} peak was also greater when classified by the true than when classified by the apparent predominant peak diameter. Men with their predominant peak in the HDL_{3b} interval had significantly greater plasma concentrations of triglycerides and apolipoprotein B and significantly lower plasma concentrations of HDL-cholesterol and apolipoprotein A-I. These results suggest that diameter of the major HDL peak may identify persons with high risk lipoprotein profiles.

As pointed out by Blanche et al. (1), the HDL_{3a} and HDL_{3b} peaks appear to correspond to the HDL_{3L} and HDL_{3D} subfractions, respectively, defined by Patch et al. (11). The untransformed gels underestimate the proportion of men with a predominant HDL_{3b} peak. When plotted against migration distance, only 14.4% of the men in our sample had their maximum peak in the HDL_{3b} interval. In contrast, determining the predominant peak directly on the particle size scale showed that 43.3% had

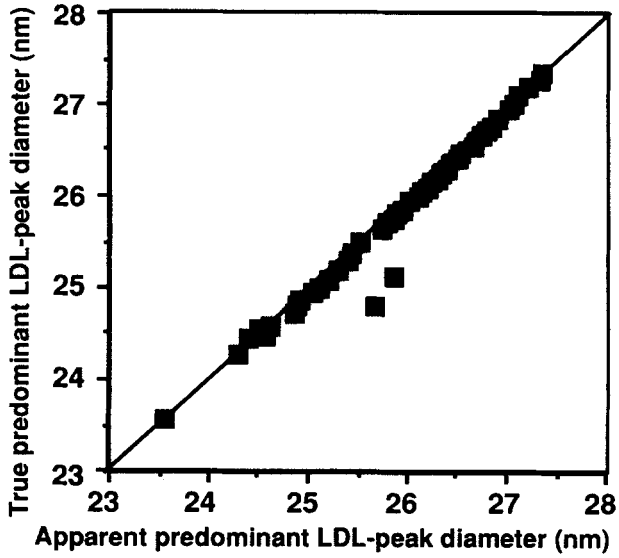

Fig. 10. Scatterplot of 97 men showing that the apparent and true predominant LDL peak diameters are usually the same.

their maximum peak in the HDL_{3b} interval. Thus 28 men (29%) were misclassified as having their predominant peak in the HDL_{3a} interval by the apparent predominant peak diameter.

Although the diameter of the apparent predominant peak is the most frequently reported HDL gel characteristic (1, 10, 12–14), other characteristics have been used. Some studies report the percent of the total HDL that falls within specified intervals (15). These percentages are not affected by the nonlinear relationship between pore diameter and migration distance, i.e., the area between two diameters is equal to the area between the corresponding migration distances. Others report the relative heights of the separate modes (13, 16) and the area under the curve as measured between the two lowest points on either side of the peak (17). Both measurements will be affected by the nonlinear relationship between pore diameter and migration distance. As shown in Fig. 5 and Fig. 8, the heights of the HDL_{3a} and HDL_{2b} peaks are overestimated when the HDL distribution is plotted against migration distance. The re-expression of the HDL distribution in terms of apparent molecular weight (18) or nonhydrated particle diameter (10) does not eliminate the need to adjust the height of the distribution.

Most studies of HDL and LDL subclasses by gradient gel electrophoresis either plot the HDL distribution versus the diameter equivalent of the migration distances, or they present the apparent diameters of the lipoprotein peaks. Additional computational effort is required to transform the distributions into the diameter scale, and this probably contributed to its avoidance. Nevertheless, the effort appears warranted given the rather substantial changes it produces in the shape of the distribution, affecting not only the relative heights of the lipoprotein peak but also their correlations with other variables.

This work was supported in part by grants HL-24462, HL-02183, and HL-18574 from the National Heart, Lung, and Blood Institute. Analytic ultracentrifuge measurements were made by the staff of the Donner Laboratory under the direction of Dr. Frank Lindgren. We wish to thank Dr. Marcia Stefanick for her help in collecting the data, Laura Glines for the analysis of the gradient gels, Dr. John Albers for apolipoprotein analyses, and Patricia Blanche, Elaine Gong, and Stephen Bicknese for their help.

Manuscript received 31 May 1989, in revised form 8 September 1989, in re-revised form 8 November; accepted 8 February 1990.

REFERENCES

1. Blanche, P. J., E. L. Gong, T. M. Forte, and A. V. Nichols. 1981. Characterization of human high density lipoproteins by gradient gel electrophoresis. *Biochim. Biophys. Acta.* **665:** 408–419.
2. Krauss, R. M., and D. J. Burke. 1982. Identification of multiple subclasses of plasma low density lipoproteins in normal humans. *J. Lipid Res.* **23:** 97–104.
3. Wood, P. D., M. L. Stefanick, D. M. Dreon, B. Frey-Hewitt, S. C. Garay, P. T. Williams, H. R. Superko, S. P. Fortmann, J. J. Albers, K. M. Vranizan, N. M. Ellsworth, R. B. Terry, and W. L. Haskell. 1988. Changes in plasma lipids and lipoproteins in overweight men during weight loss through dieting as compared with exercise. *N. Engl. J. Med.* **319:** 1173–1179.
4. Metropolitan Life Insurance Co. 1959. New weight standards for men and women. Statistical Bulletin, New York, Nov.-Dec.
5. Lipid Research Clinics Manual of Laboratory Operations. 1974. Volume 1. 1974 Lipid and Lipoprotein Analysis. HEW Publication No. NIH 75-628. U. S. Government Printing Office, Washington, DC.
6. Albers, J. J., V. G. Cabana, and W. R. Hazzard. 1975. Immunoassay of human plasma apolipoprotein B. *Metabolism.* **24:** 1339–1351.
7. Cheung, M. C., and J. J. Albers. 1977. The measurement of apolipoproteins A-I and A-II levels in men and women by immunoassay. *J. Clin. Invest.* **60:** 43–50.
8. Lindgren, F. T., L. C. Jensen, and F. T. Hatch. 1972. The isolation of quantitative analysis of lipoproteins. *In* Blood Lipids and Lipoproteins: Quantitation, Composition and Metabolism. G. J. Nelson, editor. Wiley-Interscience, New York. 181–274.
9. Hoel, P. G., S. C. Port, and C. J. Stone. 1971. Introduction to Probability Theory. Houghton Mifflin Co., Boston. 117.
10. Chen, C., K. Applegate, W. C. King, J. A. Glomset, K. R. Norum, and E. Gjone. 1984. A study of the small molecular spherical high density lipoproteins of patients afflicted with familial lecithin:cholesterol acyltransferase deficiency. *J. Lipid Res.* **25:** 269–282.
11. Patsch, W., G. Schonfeld, A. M. Gotto, and J. R. Patsch. 1980. Characterization of human high density lipoproteins by zonal ultracentrifugation. *J. Biol. Chem.* **255:** 3178–3185.
12. Hopkins, G. J., and P. J. Barter. 1986. Role of triglyeride-rich lipoproteins and hepatic lipase in determining the particle size and compositions of high density lipoproteins. *J. Lipid Res.* **27:** 1265–1277.
13. Clifton, P. M., P. J. Barter, and A. M. Mackinnon. 1988. High density lipoprotein size distribution in subjects with obstructive jaundice. *J. Lipid Res.* **29:** 121–135.
14. Chang, L. B. F., C. J. Hopkins, and P. J. Barter. 1985. Particle size distribution of high density lipoproteins as a function of plasma triglyceride concentrations in human subjects. *Atherosclerosis.* **56:** 61–70.
15. Griffin, B. A., E. R. Skinner, and R. J. Maughan. 1988. Plasma high density lipoprotein subfractions in subjects with different coronary risk indices as assessed by plasma lipoproteins concentrations. *Atherosclerosis.* **70:** 165–169.
16. Jackson, R. L., R. L. Barnhart, and M. L. Kashyap. 1987. Characterization of high density lipoproteins from patients with severe hypertriglyceridemia. *Atherosclerosis.* **66:** 37–43.
17. Cheung, M. C., and A. C. Wolf. 1988. Differential effect of ultracentrifugation on apolipoprotein A-I-containing lipoprotein subpopulations. *J. Lipid Res.* **29:** 15–25.
18. Vezina, C. A., R. W. Milne, P. K. Weech, and Y. L. Marcel. 1988. Apolipoprotein distribution in human lipoproteins separated by polyacrylamide gradient gel electrophoresis. *J. Lipid Res.* **29:** 573–585.